Ab Initio Treatment of the Chemical Reaction Precursor Complex Br(^{2}P)−HCN. 1. Adiabatic and Diabatic Potential Surfaces†

Anna V. Fishchuk,§ Jeremy M. Merritt,‡,|| and Ad van der Avoird*,§

Theoretical Chemistry, IMM, Radboud University Nijmegen, Toernooiveld 1, 6525 ED Nijmegen, The Netherlands, and Department of Chemistry, University of North Carolina, Chapel Hill, North Carolina 27599

Received: December 11, 2006; In Final Form: April 18, 2007

The three adiabatic potential surfaces of the Br(^{2}P)−HCN complex that correlate to the ^{2}P ground state of the Br atom were calculated ab initio. With the aid of a geometry-dependent diabatic mixing angle, also calculated ab initio, these adiabatic potential surfaces were transformed into a set of four diabatic potential surfaces required to define the full 3×3 matrix of diabatic potentials. Each of these diabatic potential surfaces was expanded in terms of the appropriate spherical harmonics in the atom-linear molecule Jacobi angle θ. The dependence of the expansion coefficients on the distance R between Br and the HCN center of mass and on the CH bond length was fit to an analytic form. For HCN in its equilibrium geometry, the global minimum with $D_e = 800.4$ cm^{-1} and $R_e = 6.908a_0$ corresponds to a linear Br−NCH geometry, with an electronic ground state of Σ symmetry. A local minimum with $D_e = 415.1$ cm^{-1}, $R_e = 8.730a_0$, and a twofold degenerate Π ground state is found for the linear Br−HCN geometry. The binding energy, D_e, depends strongly on the CH bond length for the Br−HCN complex and much less strongly for the Br−NCH complex, with a longer CH bond giving stronger binding for both complexes. Spin−orbit coupling was included and diabatic states were constructed that correlate to the ground $^2P_{3/2}$ and excited $^2P_{1/2}$ spin−orbit states of the Br atom. For the ground spin−orbit state with electronic angular momentum $j = (^3/_2)$ the minimum in the potential for projection quantum number $\omega = \pm(^3/_2)$ coincides with the local minimum for linear Br−HCN of the spin-free case. The minimum in the potential for projection quantum number $\omega = \pm(^1/_2)$ occurs for linear Br−NCH but is considerably less deep than the global minimum of the spin-free case. According to the lowest spin−orbit coupling included adiabatic potential the two linear isomers, Br−NCH and Br−HCN, are about equally stable. In the subsequent paper, we use these potentials in calculations of the rovibronic states of the Br−HCN complex.

1. Introduction

The weakly bound complexes X−HY with electronegative atoms or groups X, Y = F, Cl, Br, O, OH, CN occur in the entrance and exit channels of the hydrogen exchange reactions X + HY → HX + Y. It appeared experimentally[1] in the reaction of Cl with HD and theoretically[2] in the reaction Cl + OH → HCl + O that this occurrence may have significant effects on the rate of the reaction, on the product branching ratios, and so forth. Therefore, it is important to know the stability and structure of these weakly bound complexes. Experimentally, a series of these radical complexes was investigated by Merritt et al.[3,4] They were prepared in cold superfluid helium clusters in a supersonic molecular beam setup and studied by high-resolution infrared spectroscopy in the range of the HY stretch frequency. Theoretically, some of these complexes were investigated by Meuwly and Hutson,[5,6] who used empirical potentials. Our group[7−10] made detailed studies of the bound states and spectra of Cl−HCl and Cl−HF on the basis of ab initio potentials. A complex that was recently studied spectroscopically by Merritt et al.[4] is Br−HCN. This species is particularly interesting because it was found to occur in two isomeric forms: Br−HCN and Br−NCH, both linear.

Theoretical investigations on the open-shell species X(^{2}P)−HY with halogen atoms X = F, Cl, Br in their ^{2}P ground state are complicated because of electronic degeneracies, which lead to the breakdown of the Born−Oppenheimer approximation. Multiple electronic states that are asymptotically degenerate have to be included simultaneously, and the nonadiabatic coupling between these states must be taken into account. In ref 11, building on earlier work by Alexander[12] and by Dubernet and Hutson,[13,14] we described a diabatic model in which this is taken care of. The diabatic states of the complex labeled P_{-1},P_0,P_1 correlate to the spatial components of the threefold degenerate X(^{2}P) atomic ground state. Spin−orbit coupling is included as well, and a new set of diabatic states is constructed that correlates asymptotically with the X(^2P_j) states with $j = (^3/_2)$ and $j = (^1/_2)$. The diabatic potentials are obtained from three adiabatic potential surfaces $V_1(A')$, $V_2(A')$, $V(A'')$ for states of reflection symmetry A' and A'' through symmetry adapted diabatic states labeled P_x,P_y,P_z that are easily transformed into the complex states P_{-1},P_0,P_1. The symmetry adapted diabatic state P_y coincides with the adiabatic state of A'' symmetry. Only

† Part of the "Roger E. Miller Memorial Issue".

* Corresponding author. E-mail: A.vanderAvoird@theochem.ru.nl.

‡ Present address: Department of Chemistry, Emory University, Atlanta, GA 30322.

§ Radboud University Nijmegen.

|| University of North Carolina.

10.1021/jp068495n CCC: $37.00
Published on Web 06/14/2007

a single mixing angle, γ, transforming the two adiabatic states of A' symmetry into the diabatic states P_x,P_z of the same symmetry, is needed to obtain the full 3×3 matrix of complex diabatic potential surfaces $V_{\mu',\mu}$ with $\mu',\mu = -1,0,1$. In the present two papers (henceforth called paper 1 and paper 2), we applied this method to the Br−HCN complex. Paper 1 describes the ab initio calculation and analytic fit of the potential surfaces; paper 2 describes the application of the diabatic potentials in a computation of the rovibronic states and properties of the complex, with the inclusion of spin−orbit coupling. Paper 2 also includes a comparison of the ab initio computed results with the spectroscopic data.[4]

The computation and analytic fit of the potentials is described in Section 2 of paper 1. The adiabatic potentials $V_1(A')$, $V_2(A')$, $V(A'')$ were obtained from the partially spin-restricted coupled cluster [RCCSD(T)] method including single and double excitations and, noniteratively, triples.[15] To obtain the mixing angle, γ, we performed complete active space self-consistent field (CASSCF) plus multireference configuration interaction (MRCI) calculations that provided the wave functions from which this mixing angle was extracted. After transformation to the diabatic potentials, $V_{\mu',\mu}$, the latter were expanded in the appropriate spherical harmonics, according to the theory in ref 11. The dependence of the expansion coefficients on the CH bond length, r_{CH}, in the HCN monomer and on the distance R between the Br nucleus and the center of mass of HCN was fitted analytically. In Section 3, we discuss these potentials. In Section 4, we construct new diabatic states by inclusion of the important spin−orbit coupling on the Br atom and we discuss the effect of spin−orbit coupling on the diabatic and adiabatic potentials.

2. Computation and Fits of the Potential Surfaces

Three-dimensional nonrelativistic adiabatic potential energy surfaces were obtained from RCCSD(T) calculations in an atomic orbital basis of augmented correlation-consistent polarized-valence functions of double-ζ quality (aug-cc-pVDZ),[16,17] supplemented with a {332} set of uncontracted bond functions (exponents sp:0.9,0.3,0.1 and d:0.6,0.2) centered halfway between the Br nucleus and the center of mass of HCN. The equilibrium geometries of the complex were also investigated with the corresponding triple- and quadruple-ζ (aug-cc-pVTZ and aug-cc-pVQZ) basis sets, with the same midbond functions. The 1s electrons on C and N and the 1s,2s,2p,3s,3p,3d electrons on Br were left uncorrelated. The computer program molpro[18] was used in all of the calculations. The origin of a Cartesian frame was chosen on the Br nucleus, and the positive z axis along the vector **R** that points from the Br nucleus to the center of mass of HCN. The atomic masses are: $m_H = 1.0078250321$ u, $m_C = 12$ u, and $m_N = 14.0030740052$ u. To examine the experimentally observed[4] red shift in the CH stretch frequency due to the complex formation, we varied the CH bond length, r_{CH}, but froze the CN bond at the calculated equilibrium distance of $r_{CN} = 2.2220a_0$ and kept HCN linear. The vector **r**, which points from the N to the H nucleus, lies in the xz plane of the frame and makes an angle θ with the positive z axis. Hence, $\theta = 0°$ corresponds to the linear Br−NCH conformation and $\theta = 180°$ corresponds to linear Br−HCN. The coordinates that were varied in addition to r_{CH} are R, the length of the vector **R**, and the angle θ. The calculations were carried out on a $16 \times 12 \times 5$-dimensional grid. The R values were 4.5, 5.0, 5.5, 6.0, 6.5, 7.0, 7.5, 8.0, 8.5, 9.0, 9.5, 10.0, 12.5, 15.0, 20.0, and $25.0a_0$. For θ we used a 12-point Gauss−Legendre quadrature grid, and the r_{CH} grid includes the following values: 1.6661, 1.8551, 2.0440, 2.2330, and $2.4220a_0$. The value $r_3 = 2.0440a_0$ is the equilibrium CH bond length in a geometry optimization of HCN at the CCSD(T)/aug-cc-pVDZ level. The other grid values correspond to an increase/decrease of r_{CH} in steps of 0.1 Å. The values $r_1 = 1.6661a_0$ and $r_5 = 2.4220a_0$ are well beyond the classical turning points of the first excited ($v = 1$) CH stretch state.

The Br−HCN dimer with HCN kept linear is of C_s symmetry and possesses three potential energy surfaces that correlate to the ^2P ground state of the free bromine atom: two of A' symmetry (correlating to mixed P_x and P_z substates of Br) and one of A'' symmetry (correlating to P_y). The potentials $V_1(A')$ and $V(A'')$ correspond to the ground states of the two symmetries, but the potential $V_2(A')$ corresponds to an excited A' state. The RCCSD(T) method is normally used only to obtain ground-state energies. The procedure to obtain the potential $V_2(A')$ from RCCSD(T) calculations is described in ref 9. Also, the procedure to correct the interaction energies for the basis set superposition error (BSSE), which is nontrivial especially for the two A' states, is described in detail in ref 9.

In a few of the grid points, the RCCSD iterations did not converge. The $V(A'')$ potential did not cause any problems; all points gave convergence. However, for the $V_1(A')$ potential about 0.1% of the points and for the $V_2(A')$ potential about 3% of the points did not converge. The values of the potentials at these points were obtained from neighboring points by interpolation. For interpolation in the R coordinate, we used the reproducing kernel Hilbert space (RKHS)[19] method with a kernel for distancelike variables; for interpolation in r_{CH} and θ we used quadratic functions. The accuracy of these interpolations was checked by applying them to similar points for which converged RCCSD(T) interaction energies were available. Moreover, we checked this accuracy by simultaneous interpolation in more than one of the coordinates. In general, we can say that possible errors caused by interpolation are comparable with or smaller than the errors in the analytic fit. The latter are given at the end of this section.

The wave functions of the three adiabatic states $\Psi_1(A')$, $\Psi_2(A')$, and $\Psi(A'')$ needed to compute the mixing angle, γ, were obtained from CASSCF plus MRCI calculations on the same grid and with the same basis. The angle γ was obtained for each grid point from the matrix elements of the electronic angular momentum operator, L_z

$$\gamma(R, \theta, r_{CH}) = \arctan\left[\frac{\langle\Psi(A'')|L_z|\Psi_2(A')\rangle}{\langle\Psi(A'')|L_z|\Psi_1(A')\rangle}\right] \qquad (1)$$

This expression, proposed by Alexander,[12] was used earlier in studies on H_2O,[20] Cl−HCl,[21] and Cl−HF.[9] The transformation from the adiabatic potentials to the diabatic ones, with the use of this mixing angle γ, is described in detail in ref 9. The 3×3 Hermitian matrix of diabatic potentials contains four different potential surfaces: $V_{0,0}$, $V_{1,1} = V_{-1,-1}$, $V_{1,-1}$, and $V_{0,1} = -V_{0,-1}$.

As shown in ref 11, the diabatic potentials can be expanded in spherical harmonics $C^L_\mu(\theta,0)$, which are Racah-normalized such that $C^L_\mu(0,0) = \delta_\mu,0$

$$V_{\mu',\mu}(R,\theta,r_{CH}) = \sum_{L=|\mu'-\mu|}^{L_{max}} C^L_{\mu-\mu'}(\theta,0)v^L_{\mu',\mu}(R,r_{CH}) \qquad (2)$$

The expansion coefficients were calculated by numerical integration, according to eq 9 of ref 9. We used the 12-point

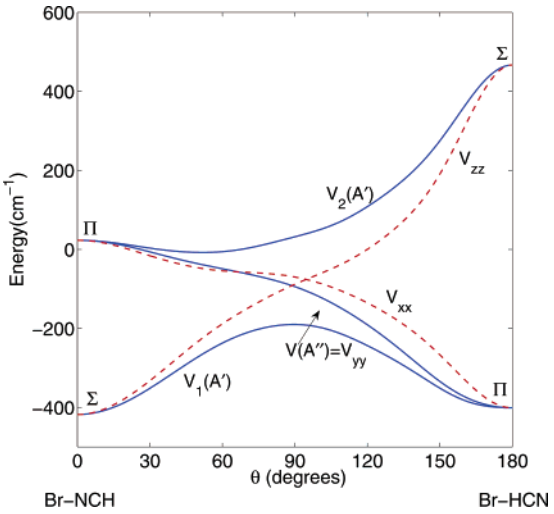

Figure 1. Three adiabatic (full) and diabatic (dashed) curves as functions of θ for $r_{CH} = 2.0440a_0$ and $R = 8.5a_0$. The diabatic curve V_{yy} coincides with the adiabatic curve $V(A'')$.

Gauss−Legendre quadrature grid in the angle θ on which the ab initio data were computed. Just as in ref 9, the expansion coefficients $v^L_{\mu',\mu}(R,r_{CH})$ were obtained as functions of R and r_{CH} by application of the RKHS method[19] to the points in the R and r_{CH} grids, with the use of a two-dimensional kernel for distancelike variables. The parameters m_{RKHS} and n_{RKHS} were chosen in the same way as in ref 9.

Because for the smallest values of R the potential becomes extremely repulsive especially at the linear Br−HCN geometry, one would need very many terms in the spherical harmonic expansion of eq 2. To avoid this, the diagonal potentials $V_{0,0}$ and $V_{1,1}$ were damped in these strongly repulsive regions by means of a tanh function up to a value V_{max}

$$\tilde{V}_{i,i} = \begin{cases} V_{i,i} & \text{for } V_{i,i} \le V_0 \\ V_0 + \beta^{-1} \tanh\left[\beta(V_{i,i} - V_0)\right] & \text{for } V_{i,i} > V_0 \end{cases} \quad (3)$$

where $\beta \equiv [V_{max} - V_0]^{-1}$. With this scheme, the damped potentials $\tilde{V}_{i,i}$ are continuous around V_0 up to the second derivative. Care was taken to use sufficiently high values of V_0 and V_{max} so that the potentials were affected only in regions that are not of any practical importance in bound-state and low-energy scattering calculations. The actual values used were $V_0 = 10\,000$ cm^{-1}, and $V_{max} = 2V_0$. At those grid points where the diagonal potentials were damped, the off-diagonal potential, $V_{0,1}$, was scaled by the factor $\tilde{V}_{0,0}/V_{0,0}$ and the off-diagonal potential, $V_{1,-1}$, by the factor $\tilde{V}_{1,1}/V_{1,1}$.

To check the quality of the fits, we used the analytically expressed diabatic potentials and recomputed the lowest adiabatic potential by diagonalization of the 3×3 matrix of diabatic potentials. When we compared that with the original ab initio points for this adiabat, we found a root-mean-square relative deviation of 1.8% in the short range for $R = 5a_0$, 0.5% in the region of the minimum for $R = 8.5a_0$, and 1.3% in the long range for $R = 12.5a_0$.

3. Results and Discussion

All plots of the potentials shown in the figures are cuts at the calculated equilibrium distance $r_{CH} = 2.0440a_0$ of HCN, which is close to the experimental value $r_{CH} = 2.0135a_0$. Figure 1 shows plots of the adiabatic and diagonal diabatic potentials as functions of the angle θ. Although the distance R is not optimized in this figure but is fixed at $R = 8.5a_0$, one can already see that both linear structures are minima. One also observes how the Br−HCN interaction splits the Br(^{2}P) state for the linear geometries into a Σ and a Π state. For linear Br−NCH ($\theta = 0°$), the Σ state is lowest in energy, whereas for linear Br−HCN ($\theta = 180°$) the Π state is lowest. This holds for the entire range of the R variable. The adiabatic A'' state always correlates with one of the Π states, whereas the other Π component corresponds to the higher adiabatic potential $V_2(A')$ for $\theta = 0°$ and to the lower adiabatic potential $V_1(A')$ for $\theta = 180°$. Bending the complex away from the linear equilibrium geometries lifts the degeneracy of the Π states and gives rise to a splitting of the corresponding adiabatic states, which increases quadratically when θ increases from 0° or decreases from 180°. Such a degeneracy gives rise to a nonadiabatic Renner−Teller coupling.[22] Because the Π state is the ground state for linear Br−HCN, we expect to see the effects of this coupling in the lower rovibronic levels of this complex. This was indeed found and will be discussed in paper 2.

Figure 2 shows contour plots of the adiabatic potentials as functions of R and θ. The two prominent minima in $V_1(A')$ corresponding to the two different linear configurations Br−NCH and Br−HCN are clearly visible. The Br−NCH global minimum in the fit of the potential has $D_e = 800.4$ cm^{-1} and $R_e = 6.908a_0$. The minimum for linear Br−HCN is a local minimum with $D_e = 415.1$ cm^{-1} and a much larger equilibrium distance $R_e = 8.730a_0$. As discussed above, the Br−HCN minimum coincides with the minimum in the potential $V(A'')$ and corresponds to a Π electronic ground state.

These minima were also computed with the larger aug-cc-pVTZ and aug-cc-pVQZ bases, supplemented with the same bond functions as the aug-cc-pVDZ basis used for all geometries. The ab initio values of D_e at the global minimum for linear Br−NCH are 790, 737, and 850 cm^{-1} for the aug-cc-pVDZ, aug-cc-pVTZ, and aug-cc-pVQZ bases, respectively. If the HCN monomer geometry is reoptimized at the aug-cc-pVTZ level, then the D_e value with this basis becomes 749 cm^{-1}. Fortuitously, for the aug-cc-pVDZ basis used this value seems even better than that for the aug-cc-pVTZ basis. The D_e values at the local minimum for linear Br−HCN, which are 415, 425, and 430 cm^{-1}, respectively, are very similar for the different basis sets. Also, the energies of the higher states, the Π state for linear Br−NCH and the Σ state for linear Br−HCN, are very similar in the three bases.

Figure 3 shows contour plots of the diabatic potentials. The potential $V_{0,0} = V_{zz}$ corresponds to a Σ state for both linear geometries. Its minimum for linear Br−NCH coincides with that in $V_1(A')$. The potential $V_{1,1} = (V_{xx} + V_{yy})/2$, which has a minimum for linear Br−HCN, corresponds to the Π state for the linear geometries. It looks quite similar to the $V(A'')$ adiabat also for nonlinear structures, which is not surprising because $V(A'') = V_{yy}$ and V_{xx} is very similar to V_{yy}, cf. Figure 1. The latter implies that $V_{1,-1} = (V_{yy} - V_{xx})/2$ (not shown) is very small. The off-diagonal diabatic potential $V_{0,1} = -V_{xz}/\sqrt{2}$ is much more significant, especially near $\theta = 30°$ and 140°; see the lower panel in Figure 3.

Variation of the distance r_{CH} does not change the potentials qualitatively. Quantitative differences can be observed in Table 1, where we present D_e and R_e values for each of the five r_{CH} points used for the ab initio calculations. For the Br−NCH complex, D_e increases with increasing r_{CH} distance, but only slightly. For the Br−HCN complex, however, D_e and R_e are

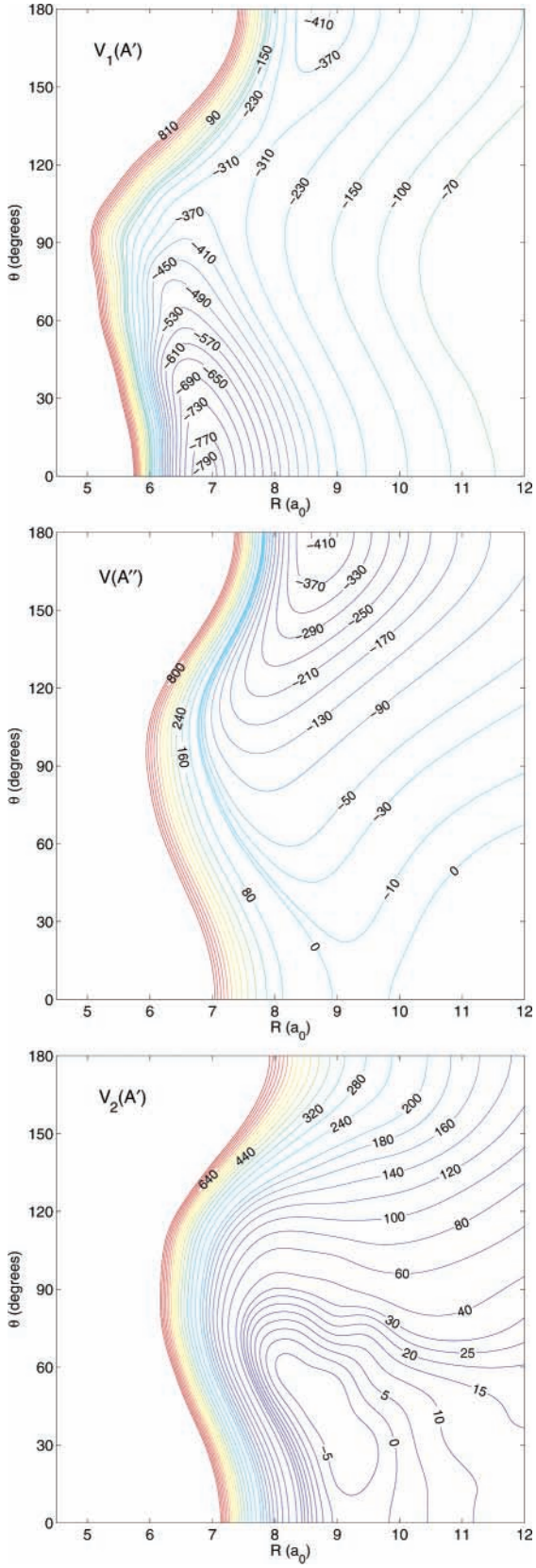

Figure 2. Adiabatic potential surfaces $V_1(A')$, $V(A'')$, and $V_2(A')$ (in cm^{-1}) for $r_{CH} = 2.0440a_0$.

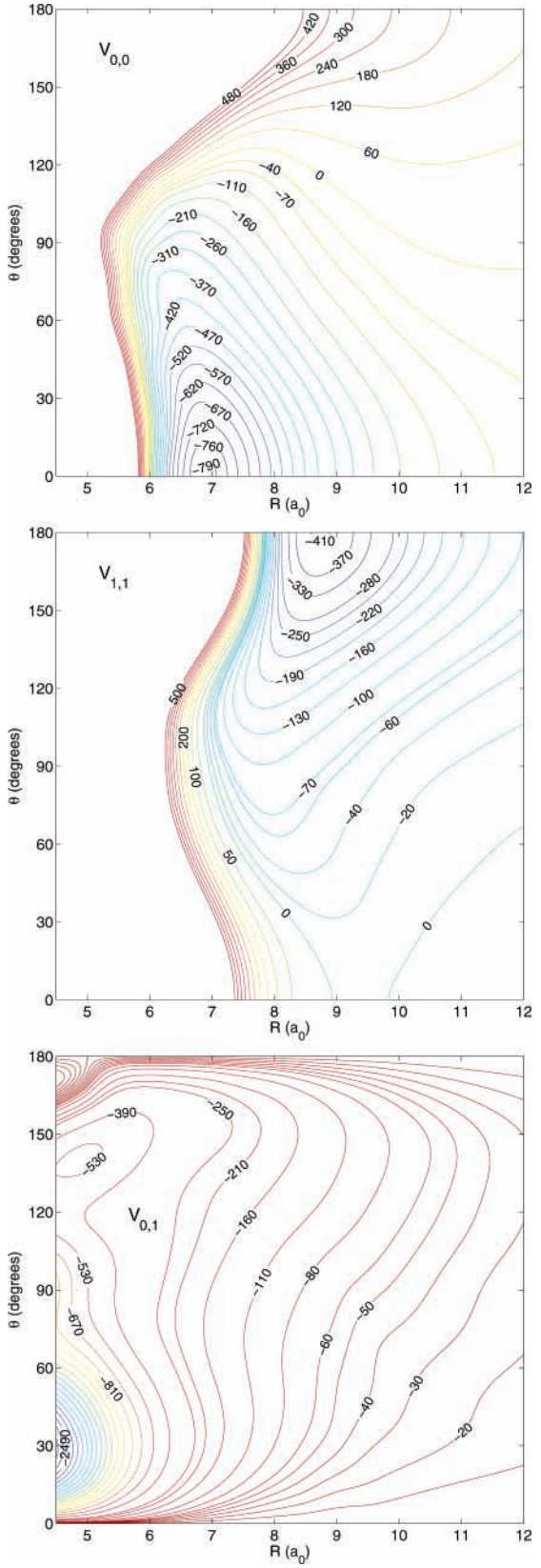

Figure 3. Diabatic potential surfaces $V_{0,0}$, $V_{1,1}$, and $V_{0,1}$ (in cm^{-1}) for $r_{CH} = 2.0440a_0$.

much more sensitive to variation of r_{CH}. This is what might be expected from the structures of the two complexes.

The fact that linear Br−HCN has a ground state of Π symmetry, whereas linear Br−NCH has a Σ ground state can be well understood from electrostatic considerations. The Br atom in its ^2P ground state has a large quadrupole moment. The interaction of this quadrupole with the dipole of HCN is the dominant contribution to the interaction energy. The Σ and Π components of this quadrupole moment are the expectation values of the quadrupole operator $Q_{2,0} = \sum_i r_i^2 C_{2,0}(\theta_i,\phi_i)$ over

TABLE 1: Dependence of the Well Depth, D_e, and the Equilibrium Distance, R_e, on r_{CH} for Linear Br−NCH on the Lowest Adiabatic Surface $V_1(A')$ Corresponding to the Σ State and for Linear Br−HCN on the Lowest Adiabatic Surfaces $V_1(A')$ and $V(A'')$ Corresponding to the Π State

	Br−NCH		Br−HCN	
r_{CH} (a_0)	R_e (a_0)	D_e (cm^{-1})	R_e (a_0)	D_e (cm^{-1})
1.6661	6.920	769.17	8.659	326.67
1.8551	6.915	785.42	8.709	364.82
2.0440	6.908	800.42	8.730	415.11
2.2330	6.887	807.41	8.724	481.39
2.4220	6.895	824.40	8.684	570.47

the Br(P_0) and Br($P_{\pm1}$) substates, respectively, where (r_i,θ_i,ϕ_i) denote the electronic coordinates. The Br atom is isoelectronic to the rare gas atom Kr with one electron taken out of the 4p shell. In the Σ state, this electron is taken out of a $4p_z$ orbital along the bond axis; in the Π state it is taken out of a $4p_1$ or $4p_{-1}$ orbital. Or, equivalently, out of $4p_x$ or $4p_y$. Therefore, it is not surprising that the Σ quadrupole has a positive value, whereas the Π state quadrupole moment is negative. The Σ quadrupole interacts most favorably with the negative N side of HCN, giving Br−NCH, the Π quadrupole interacts most favorably with the positive H side of HCN, giving Br−HCN. This agrees with the equilibrium structures found in the full ab initio calculations.

Finally, let us compare Br−HCN with some similar complexes of which the interaction potentials were recently computed ab initio. The complex Cl−HF[9,10] has a global minimum at the linear Cl−HF structure. This structure has a ground state of Π symmetry, just as linear Br−HCN. The value of D_e = 676.5 cm^{-1} for Cl−HF at the equilibrium bond length of HF is larger than that for Br−HCN. The global minimum for linear Br−NCH with its Σ electronic ground state corresponds to a local minimum with D_e = 237.4 cm^{-1} for Cl−FH. For Cl−HCl,[7,8,21] two deep minima were also found, and the minimum for linear Cl−HCl is qualitatively similar to those of linear Br−HCN and Cl−HF. The second minimum, with a Σ electronic ground state, occurs in Cl−HCl for a T-shaped structure. This is probably related to the above considerations about the dominance of electrostatic interactions. For HCl, it is usually not only the dipole that plays a role in such interactions but also the quadrupole. Interaction of this quadrupole with the quadrupole of Cl(^{2}P) leads to maximum binding for a T-shaped Cl−HCl complex. Similar T-shaped equilibrium structures were found for OH−HCl,[23] HCl−HCl,[24] and HCN−HCl.[25] For F−HF three minima were found,[26] one for each of the two linear geometries and a T-shaped one. The linear F−HF minimum was the deepest, then the T-shaped one, while the linear F−FH minimum is the shallowest. The barriers between these minima are small, however. In Br−HBr,[26] the situation is qualitatively similar to Cl−HCl: a linear Br−HBr minimum and a T-shaped minimum, with the first one being deeper. The linear Br−BrH complex corresponds to a saddle point, just as Cl−ClH.

4. Effect of Spin−Orbit Coupling

The spin−orbit states of the Br atom are split by D_{SO} = $E(^2P_{1/2}) - E(^2P_{3/2})$ = 3685.5 cm^{-1}. We assume that the spin−orbit coupling in the Br atom is not affected by the relatively weak interaction with the HCN molecule so that we may use for the Br−HCN complex the spin−orbit coupling term $A\hat{\lambda}\hat{S}$ with the operators $\hat{\lambda}$ and $\hat{S}$ representing the orbital and spin angular momenta of the Br(^{2}P) atom and the constant parameter $A = -(^2/_3)D_{SO}$. Because we expect that this large splitting has an important effect on the properties of the complex, we constructed a new set of diabatic electronic states with the inclusion of spin−orbit coupling. These states are denoted by $|j_A\omega_A\rangle$, where the quantum number j_A is the total angular momentum on the Br atom A and ω_A is the projection of j_A on the dimer axis **R**. They are obtained from the original, spin-free, diabatic states $|\lambda, \mu\rangle$ and the spin functions $|S, \sigma\rangle$ by Clebsch−Gordan coupling

$$|j_A\omega_A\rangle \equiv |(\lambda S)\, j_A\omega_A\rangle = \sum_{\mu,\sigma} |\lambda, \mu\rangle|S, \sigma\rangle\, \langle\lambda, \mu; S, \sigma|\, j_A, \omega_A\rangle \tag{4}$$

where $\langle\lambda, \mu; S, \sigma\, |j_A, \omega_A\rangle$ is a Clebsch−Gordan coefficient. Because $\lambda = 1$ and $S = (^1/_2)$, the total atomic angular momentum of Br takes on the values $j_A = (^1/_2)$ with projections $\omega_A = \pm(^1/_2)$ on the z axis and $j_A = (^3/_2)$ with projections $\omega_A = \pm(^1/_2), \pm(^3/_2)$. Diabatic states with $j_A = (^3/_2)$ correlate to the $^2P_{3/2}$ ground state of the Br atom, states with $j_A = (^1/_2)$ with the excited $^2P_{1/2}$ state. Because the atomic spin−orbit splitting is so large, the $j_A = (^1/_2)$ basis functions will probably not play a significant role in the lower rovibronic levels of the complex. Diagonal and off-diagonal spin−orbit coupled diabatic potentials, labeled with j'_A, ω'_A; j_A, ω_A, are obtained from the diabatic potentials $V_{\mu',\mu}$ in the spin-free diabatic basis $|\lambda, \mu\rangle$ by a similarity transformation according to eq 4.

Figure 4 shows the two diagonal spin−orbit diabatic potentials $V_{jA},\omega_A; j_A,\omega_A$ with $j_A = (^3/_2)$. The potential for $|\omega_A| = (^3/_2)$ has a minimum at $\theta = 180°$, which corresponds to the linear Br−HCN configuration. For linear geometries, this potential coincides with the spin-free diabatic potential $V_{1,1}$ in Figure 3 because the spin−orbit coupled state with $|\omega_A| = (^3/_2)$ contains only the spin-free diabatic states $P_\pm \equiv |\lambda, \mu\rangle$ with $\lambda = 1,\mu = \pm1$ and the diabatic coupling potential $V_{1,-1}$ vanishes for linear geometries. Also, for nonlinear geometries the spin−orbit coupled potential for $|\omega_A| = (^3/_2)$ is very similar to $V_{1,1}$ because the off-diagonal diabatic potential $V_{1,-1}$ is very small everywhere. The potential for $|\omega_A| = (^1/_2)$ has a minimum at $\theta = 0°$, which corresponds to the linear Br−NCH configuration. Such a minimum also occurs in the spin-free diabatic potential $V_{0,0}$, which is the dominant contribution to $V_{(3/2),(1/2);(3/2),(1/2)}$, but there it is considerably deeper, cf. Figure 3. This is due to the fact (which one may easily check by inspection of the Clebsch−Gordan coefficients) that the spin−orbit coupled state with $j_A = (^3/_2)$ and $|\omega_A| = (^1/_2)$ has only $^2/_3$ of P_0 ($\mu = 0$) character and $^1/_3$ of $P_{\pm1}$ ($\mu = \pm1$) character. The deep minimum in $V_{0,0}$ for linear Br−NCH is partly damped because $V_{1,1}$ is repulsive in this region. With the inclusion of spin−orbit coupling, the minimum for linear Br−HCN ($\theta = 180°$) with $|\omega_A| = (^3/_2)$ is deeper than the minimum for linear Br−NCH ($\theta = 0°$) with $|\omega_A| = (^1/_2)$, whereas without spin−orbit coupling the linear Br−NCH conformation was much more stable.

The spin−orbit coupled diabatic potentials are elements of a 6 × 6 matrix. These elements are obtained from the similarity transformation of the spin-free diabatic potentials $V_{\mu',\mu}$ according to eq 4, and the addition of $A[\, j_A(j_A + 1) - \lambda(\lambda + 1) - S(S + 1)]/2$ with $\lambda = 1$, $S = (^1/_2)$, and $j_A = (^3/_2)$ or $(^1/_2)$ on the diagonal. These diagonal terms represent the spin−orbit coupling operator $A\hat{\lambda}\hat{S} = A(\hat{j}_A^2 - \hat{\lambda}^2 - \hat{S}^2)/2$, which is diagonal in the basis $|j_A\omega_A\rangle$. Diagonalization of this 6 × 6 matrix produces spin−orbit coupling included adiabatic potentials, more briefly called

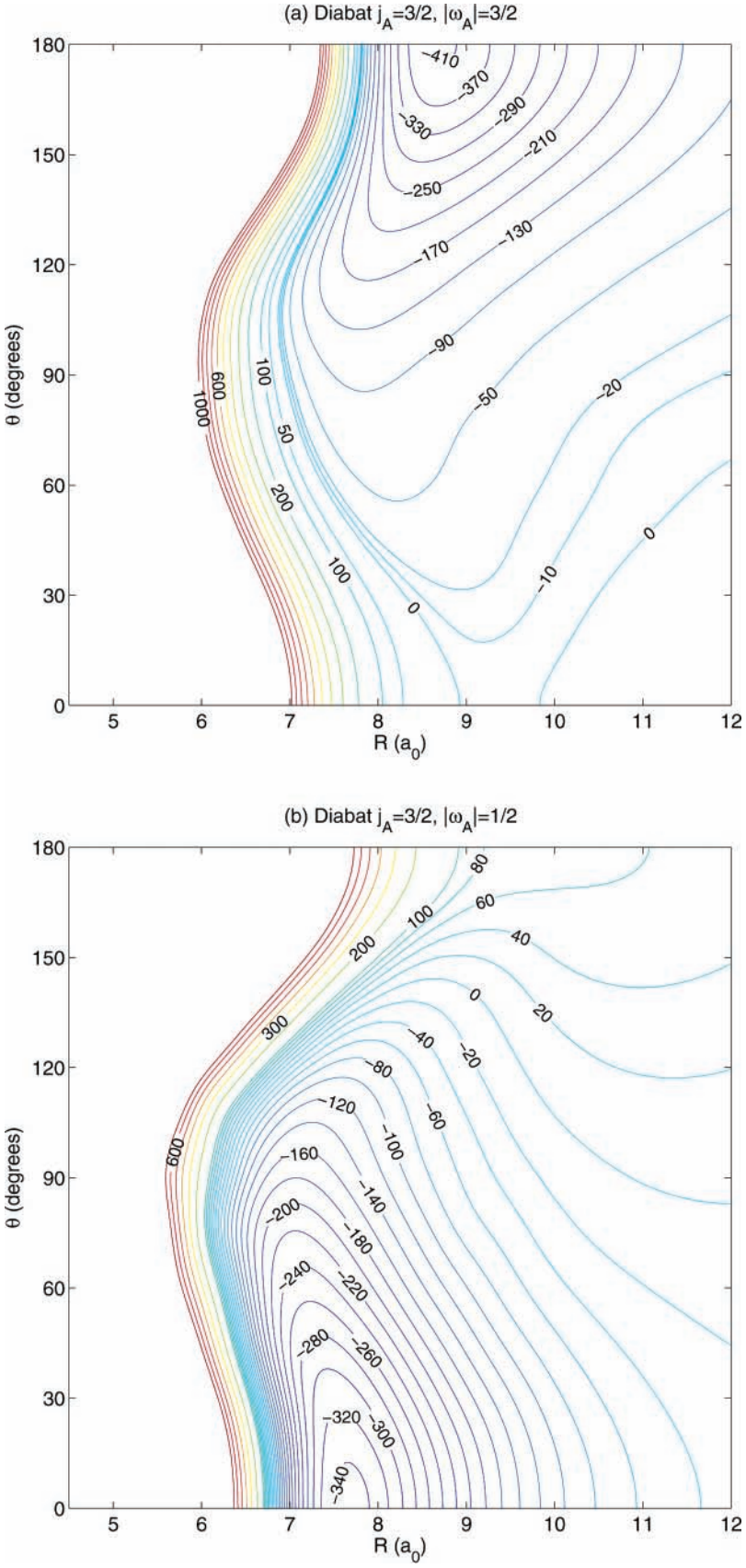

Figure 4. Diabatic potential energy surfaces including spin−orbit coupling for $j_A = (^3/_2)$. Energy (in cm^{-1}) relative to the $Br(^2P_{3/2})$ and HCN ground states.

spin−orbit adiabatic potentials. Figure 5 shows the spin−orbit adiabatic potential that is the lowest eigenvalue of this matrix, for each geometry of the complex. Here, we find both minima, one for linear Br−HCN that originates from the $j_A = |\omega_A| = (^3/_2)$ contribution and one for linear Br−NCH originating from $j_A = (^3/_2), |\omega_A| = (^1/_2)$. Because of the effect of spin−orbit

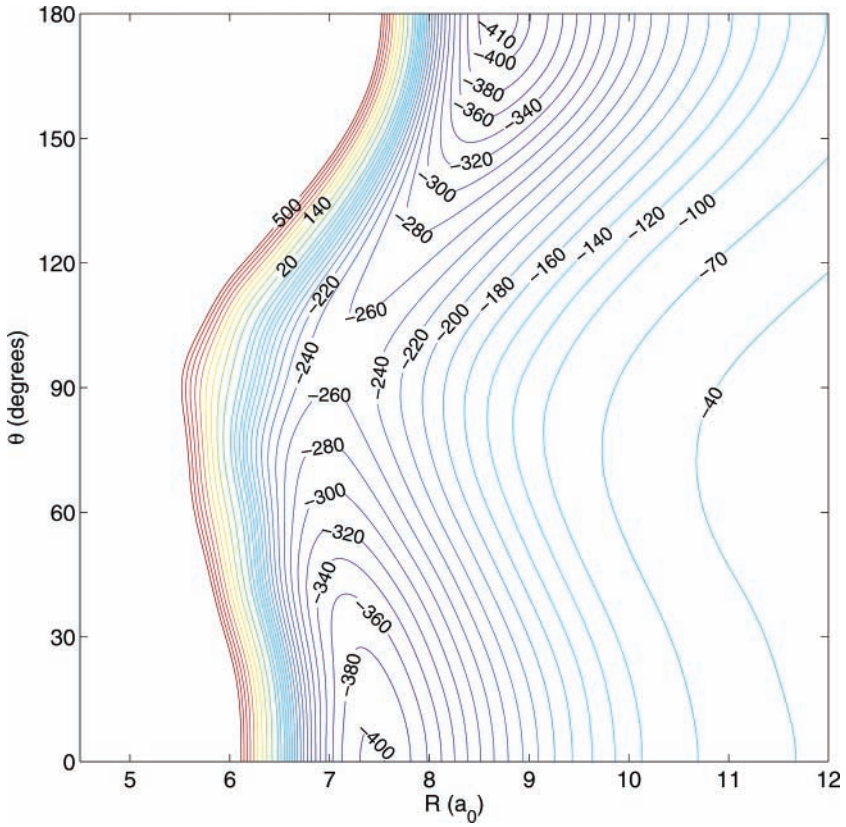

Figure 5. Lowest spin−orbit adiabatic potential energy surface. Energy (in cm^{-1}) relative to the $Br(^2P_{3/2})$ and HCN ground states.

coupling, the two minima have become about equally deep, in contrast with those in the lowest spin-free adiabatic potential in Figure 2.

5. Conclusions

The three adiabatic potentials of the Br−HCN complex that correlate to the ^2P ground state of the Br atom were calculated ab initio at the RCCSD(T) level of theory as functions of the intermolecular distance R, the atom-linear molecule Jacobi angle θ, and the length r_{CH} of the CH bond in HCN. Two of these potentials, $V_1(A')$ and $V_2(A')$, correspond to the lowest states of even (A') reflection symmetry, the third one, $V(A'')$, to the ground state of odd (A'') symmetry. From CASSCF and MRCI calculations for the same set of geometries of the complex, we obtained the corresponding wave functions and the diabatic mixing angle, γ. With the use of this mixing angle, we transformed the adiabatic states to a set of intermediate diabatic states P_x, P_z of A' symmetry and P_y of A'' symmetry, and next to the diabatic states P_{-1},P_0,P_1. The resulting potentials $V_{0,0}$, $V_{1,1} = V_{-1,-1}$, $V_{0,1} = -V_{0,-1}$, $V_{1,-1}$, which define the full 3×3 matrix of diabatic potentials and are conveniently used in bound-state calculations, were expanded in terms of the appropriate spherical harmonics in the Jacobi angle, θ. The dependence of the expansion coefficients on the Br−HCN distance R and the CH distance r_{CH} was represented in analytic form by means of the RKHS method.

In paper 2, we apply these potentials in calculations of the rovibronic states of the Br−HCN complex, in which we also include spin−orbit coupling. Here we considered the spin−orbit coupling included diabatic states used in these calculations and we showed that spin−orbit coupling has an important effect on the corresponding diabatic and adiabatic potentials.

Acknowledgment. We thank Dr. G. C. Groenenboom for stimulating discussions.

References and Notes

(1) Skouteris, D.; Manolopoulos, D. E.; Bian, W.; Werner, H.-J.; Lai, L.-H.; Liu, K. *Science* **1999**, *286*, 1713.
(2) Xie, T.; Wang, D.; Bowman, J. M.; Manolopoulos, D. E. *J. Chem. Phys.* **2002**, *116*, 7461.
(3) Merritt, J. M.; Küpper, J.; Miller, R. E. *Phys. Chem. Chem. Phys.* **2005**, *7*, 67.
(4) Merritt, J. M.; Küpper, J.; Miller, R. E. *Phys. Chem. Chem. Phys.* **2007**, *9*, 401.
(5) Meuwly, M.; Hutson, J. M. *J. Chem. Phys.* **2000**, *112*, 592.
(6) Meuwly, M.; Hutson, J. M. *J. Chem. Phys.* **2003**, *119*, 8873.
(7) Zeimen, W. B.; Kłos, J. A.; Groenenboom, G. C.; van der Avoird, A. *J. Phys. Chem. A* **2003**, *107*, 5110.
(8) Zeimen, W. B.; Kłos, J.; Groenenboom, G. C.; van der Avoird, A. *J. Phys. Chem. A* **2004**, *108*, 9319.
(9) Fishchuk, A. V.; Wormer, P. E. S.; van der Avoird, A. *J. Phys. Chem. A* **2006**, *110*, 5273.
(10) Fishchuk, A. V.; Groenenboom, G. C.; van der Avoird, A. *J. Phys. Chem. A* **2006**, *110*, 5280.
(11) Zeimen, W. B.; Kłos, J. A.; Groenenboom, G. C.; van der Avoird, A. *J. Chem. Phys.* **2003**, *118*, 7340.
(12) Alexander, M. H. *J. Chem. Phys.* **1993**, *99*, 6014.
(13) Dubernet, M.-L.; Hutson, J. M. *J. Chem. Phys.* **1994**, *101*, 1939.
(14) Dubernet, M.-L.; Hutson, J. M. *J. Phys. Chem.* **1994**, *98*, 5844.
(15) Knowles, P. J.; Hampel, C.; Werner, H.-J. *J. Chem. Phys.* **1993**, *99*, 5219.
(16) Kendall, R. A.; Dunning, T. H.; Harrison, R. J. *J. Chem. Phys.* **1992**, *96*, 6796.
(17) Woon, D. E.; Dunning, Jr., T. H. *J. Chem. Phys.* **1993**, *98*, 1358.
(18) MOLPRO is a package of ab initio programs written by H.-J. Werner and P. J. Knowles, with contributions from J. Almlöf, R. D. Amos, A. Berning, D. L. Cooper, M. J. O. Deegan, A. J. Dobbyn, F. Eckert, S. T. Elbert, C. Hampel, R. Lindh, A. W. Lloyd, W. Meyer, A. Nicklass, K. Peterson, R. Pitzer, A. J. Stone, P. R. Taylor, M. E. Mura, P. Pulay, M. Schütz, H. Stoll, and T. Thorsteinsson.
(19) Ho, T.-S.; Rabitz, H. *J. Chem. Phys.* **1996**, *104*, 2584.
(20) Dobbyn, A. J.; Knowles, P. J. *Mol. Phys.* **1997**, *91*, 1107.

(21) Kłos, J.; Chałasiński, G.; Szczęśniak, M. M.; Werner, H.-J. *J. Chem. Phys.* **2001**, *115*, 3085.
(22) Renner, R. *Z. Phys.* **1934**, *92*, 172; English translation in Hettema, H. *Quantum Chemistry: Classic Scientific* Papers; World Scientific: Singapore, 2000.
(23) Wormer, P. E. S.; Kłs, J.; Groenenboom, G. C.; van der Avoird, A. *J. Chem. Phys.* **2005**, *122*, 244325.
(24) Vissers, G. W. M.; Oudejans, L.; Miller, R. E.; Groenenboom, G. C.; van der Avoird, A. *J. Chem. Phys.* **2004**, *120*, 9487.
(25) van der Avoird, A.; Pedersen, T. B.; Dhont, G. S. F.; Fernández, B.; Koch, H. *J. Chem. Phys.* **2006**, *124*, 204315.
(26) Kłos, J.; Szczęśniak, M. M.; Chałsiński, G. *Int. Rev. Phys. Chem.* **2004**, *23*, 541.